Effect of the chiral discrimination on the vibrational properties of (R)-, (S)- and (R, S)-ibuprofen/methyl-β-cyclodextrin inclusion complexes

Vincenza Crupi, G. Guella, Domenico Majolino, I. Mancini, Alessandro Paciaroni, Barbara Rossi, Valentina Venuti, Paolo Verrocchio, Gabriele Viliani

Effect of the chiral discrimination on the vibrational properties of (R)-, (S)- and (R, S)-ibuprofen/methyl-β-cyclodextrin inclusion complexes

Journal:	*Philosophical Magazine & Philosophical Magazine Letters*
Manuscript ID:	TPHM-10-Jun-0281.R1
Journal Selection:	Philosophical Magazine
Date Submitted by the Author:	22-Jul-2010
Complete List of Authors:	Crupi, Vincenza; University of Messina, Physics Department Guella, G.; University of Trento, Physics Department Majolino, Domenico; University of Messina, Physics Department Mancini, I.; University of Trento, Physics Department Paciaroni, Alessandro; University of Perugia, Physics Department Rossi, Barbara; University of Trento, Physics; University of Trento, Physics Department Venuti, Valentina; University of Messina, Physics Department Verrocchio, Paolo; University of Trento, Physics Viliani, Gabriele; Universita' di Trento, Fisica; University of Trento, Physics Department
Keywords:	inclusions, IR, biophysics
Keywords (user supplied):	

Effect of the chiral discrimination on the vibrational properties of (R)-, (S)- and (R, S)-ibuprofen/methyl-β-cyclodextrin inclusion complexes

V. CRUPI[1], G. GUELLA[2], D. MAJOLINO[1], I. MANCINI[2], A. PACIARONI[3], B. ROSSI[2,4], V. VENUTI[*1], P. VERROCCHIO[2] and G. VILIANI[2]

[1]Dipartimento di Fisica, Università di Messina & CNISM, Viale Ferdinando Stagno D'Alcontres 31, 98166, Messina, ITALY.

[2]Dipartimento di Fisica, Università degli Studi di Trento, Via Sommarive 14, 38123 Povo, Trento, ITALY.

[3]Dipartimento di Fisica, Università degli Studi di Perugia, CEMIN e INFM CRS SOFT, Via A. Pascoli, 06123 Perugia, ITALY.

[4]Fondazione Bruno Kessler, Via Sommarive 18, 38123 Povo, Trento, ITALY.

*Corresponding author. Tel: +39-090-6765010; fax: +39-090-395004; email: vvenuti@unime.it

Abstract

The effects of chiral discrimination of ibuprofen (IBP) on the complexation process with methyl-β-cyclodextrin (Me-β-CD) have been investigated, in solid phase, by FTIR-ATR spectroscopy and numerical simulation. The inclusion mechanism has been discussed by the temperature-dependent analysis of the vibrational spectra, in the C=O stretching region, of complexes formed by Me-β-CD with the two enantiomeric and the racemic forms of IBP. It turned out to be enthalpy-driven, with IBP enantiomers giving rise to more stable inclusion complexes with respect to the racemate.

Keywords: Ibuprofen; inclusion complex ; FTIR-ATR spectroscopy; numerical simulation.

1. Introduction

Chirality is an important property of the molecules, whose study is of great interest in chemistry, biology and pharmaceutical science, also for its application in many technological fields. It expresses the property of a system to be non-invariant with respect to the reflection operation; thus, a molecule is chiral if it is non-superimposable onto its mirror image and the two non-identical mirror images are called enantiomers or optical isomers. Enantiomers have identical physical and chemical properties, so that they cannot be separated directly by any of the conventional chemical techniques; nevertheless, enantiomeric forms of the same molecule show different stereoselective interactions with many biological molecules, such as enzymes, which are chiral, leading enormous impact on biological processes. In particular, chirality plays a relevant role in drug development, since most of the drugs are chiral molecules and their enantiomers show different pharmacological activities [1]. In this context, the resolution of a racemic–mixture still remains one of the technologies applied for the commercial production of enantiomerically pure chiral compounds.

Ibuprofen (IBP, 4-isobutyl-2-phenyl-propionic acid), one of the most effective and widely used non-steroidal analgesic and anti-inflammatory agent, contains in its chemical structure a stereogenic carbon, thus it can exist in two enantiomeric forms (R)- and (S)-ibuprofen (see figure 1(a-b)).

[Insert figure 1 about here]

(R)- and (S)-IBP exhibit different pharmacological performance, in particular, only (S)-IBP is biologically active and primarily responsible for the anti-inflammatory activity of the drug. Nevertheless, IBP is currently clinically used as a racemate (R, S)-IBP form, because *in vivo* (R)-form is continuously metabolically converted into the (S)-form [2].

Structural properties of IBP enantiomers and racemate have been widely characterized, by different experimental techniques and simulation [3-11]. In particular, it was observed that in crystal lattices of both (S)- and (R, S)-IBP two molecules are arranged to form a cyclic dimer through hydrogen bonds between their carboxylic groups COOH. Thermodynamics of sublimation, crystal lattice energies, and crystal structures of racemate and enantiomers of IBP have been also characterized [4, 5] in order to understand the differences of drug-drug intermolecular interactions in the two cases. This information is the basic knowledge needed for a rational development of the appropriate method for the resolution of racemate. In particular, cyclodextrins (CDs), which are chiral macrocycles characterized by a hydrophobic inner cavity and a outer hydrophilic surface, have been used as chiral selectors for the separation of IBP enantiomers[12-15]. In this sense, a

deeper understanding of the interactions occurring between each of the two enantiomeric forms of IBP and the hydrophobic cavity of CDs is of fundamental importance. For example, it has been shown that, in liquid phase, (S)-IBP forms more stable inclusion complexes with hydroxyprophyl-β-cyclodextrin (HP-β-CD) as compared with (R, S)-IBP [16], as well as chiral discrimination was studied in water by NMR analysis. [17]. Nevertheless, a limited number of investigations on the complexes in solid state is found in literature.

Recently we have reported a study of solid inclusion complexes of (R, S)-IBP with β-cyclodextrin (β-CD) and methyl-β-cyclodextrin (Me-β-CD) by using Fourier transform infrared spectroscopy in Attenuated Total Reflectance geometry (FTIR-ATR) and Density Functional Theory (DFT) calculations. [18] The combined use of experimental and numerical techniques revealed a successful tool for the interpretation of the modifications induced in the vibrational spectra of IBP by inclusion in the CD cavity. In particular, the shifts to the higher frequencies of the FTIR band, assigned to the C=O stretch vibration, was attributed to the complexation-induced breakdown of the intermolecular hydrogen bonds in the IBP dimer. Finally, from the temperature dependent studies, the thermodynamic parameter ΔH associated to the binding of IBP with βCDs in solid phase has been estimated. From the results, Me-β-CD has been shown to be the most effective carrier for racemate IBP.

Here, we focus our attention on the inclusion complexes formed by Me-β-CD with the two enantiomers of IBP by using a temperature-dependent analysis of the vibrational properties in solid phase using FTIR-ATR spectroscopy and numerical simulation, in order to understanding if chirality of IBP can determine different interactions with CD molecules, thus influencing the complexation mechanism, i.e. geometry and/or thermal stability of inclusion complexes.

2. Experimental details and computational methods

β-cyclodextrin (β-CD) and methyl-β-cyclodextrin (Me-β-CD, degree of substitution ≈ 1.7–1.9) were purchased from Fluka Chemie (Switzerland). Racemic, (R)- and (S)-IBP were acquired from Sigma-Aldrich. All the reagents were used without purification. For the synthesis of complexes, Me-β-CD (65.5 mg, 0.05 mmol) was dissolved in water (0.5 ml) to obtain a 0.1 mM solution; subsequently, another 1 ml of water was added and the mixture was stirred at 50°C in order to obtain a limpid solution. An equimolar amount of dry (R)- (or (S)-IBP) (10.4 mg, 0.05 mmol) was added to this solution and the resulting dispersion was stirred at 50°C for 2 hours, obtaining a white dispersion. The liquid phase was removed and both the evaporated surnatant and the precipitate

were dried in a vacuum chamber, using P_2O_5 as dehydratant. Electrospray ionization mass spectrometry (ESI-MS, Bruker Esquire spectrometer) measurements and nuclear magnetic resonance (NMR, Bruker Avance 400 sectrometer) analysis allowed to verify the effective complex formation and to obtain information its stoichiometry, that turned out to be 1:1 [19].

FTIR-ATR absorption measurements were performed, from 250 K to 340 K, in the 400 ÷ 4000 cm^{-1} wavenumber range. Spectra were recorded using a Bomem DA8 Fourier transform spectrometer, operating with a Globar source, in combination with a KBr beamsplitter and a thermoelectrically cooled deuterated triglycene sulphate (DTGS) detector. The powders were contained in Golden Gate diamond ATR system, just based on the Attenuated Total Reflectance (ATR) technique. The spectra were recorded with a resolution of 4 cm^{-1}, automatically adding 100 repetitive scans in order to obtain a good signal-to-noise ratio and highly reproducible spectra. All the measurements were performed in a dry atmosphere. All the spectra were normalized for taking into account the effective number of absorbers. No smoothing was done, and spectroscopic manipulation such as baseline adjustment and normalization were performed using the Spectracalc software package GRAMS (Galactic Industries, Salem, NH, USA). The analysis of the 1500 ÷ 1800 cm^{-1} region, typical of the C=O stretching vibrational mode, that required a band decomposition procedure, was undertaken using the curve fitting routine provided in the PeakFit 4.0 software package, which enabled the type of fitting function to be selected and allowed specific parameters to be fixed or varied accordingly. Preliminarly, second derivative computations have been used for evaluating the wavenumbers of the maxima of the different sub-bands, and the fitting procedure was applied to the experimental profiles based on these wavenumber values. The strategy adopted was to use well-defined shape components of Voigt functions with all the parameters allowed to vary upon iteration. The statistical parameters were used as a guide to "best-fit". The procedure adopted makes use of the minimum number of parameters. The best-fit is characterized by $r^2 \sim 0.99$ for all the investigated systems.

Starting structures of the two enantiomeric and the racemic forms of IBP molecule were generated connecting by hydrogen bonds the carboxylic groups of (R)- (or (S)-IBP) single molecules by using PCMODEL 7.0 (Serena Software, Bloomington, Indiana) and the resulting structures minimized using molecular mechanics methods. Subsequently, this initial geometry was re-optimised at B3LYP level, using standard basis set 6-31G implemented in Gaussian 03W revision C.02 program package [20,21,22] and the optimised structural parameters were used in energy calculations at Density Functional Theory (DFT) levels.

3. Results and discussion

In figure 2(a-c) the FTIR-ATR spectra of (R, S)-, (R)- and (S)-IBP are shown in the whole explored wavenumer range, 600 ÷ 3800 cm^{-1}. The C=O stretching region (1500 ÷ 1800 cm^{-1}) was investigated in detail, since, being this vibration very active in the infrared, it can constitute an excellent candidate to reveal variations in peak-intensity, frequency and shape, attributable to the complexation process. The corresponding FTIR-ATR spectra in the region of C=O stretching vibration are reported in the inset of figure 2. The major differences appear when comparing the spectra of the two enantiomers with that of the racemate IBP, while minor changes occur between the (R)- and (S)-IBP spectra.

[Insert figure 2 about here]

The observed differences in the vibrational dynamics can be explained by taking into account the different symmetry exhibited by the racemate and the two enantiomeric forms of IBP. As specified in the Introduction, and based on our previous FTIR-ATR and quantum chemical results [18,19], uncomplexed IBP prevalently develops dimeric entities derived from symmetric hydrogen bonding of the two carboxylic groups of adjacent molecules. However, as it turns out from molecular mechanics calculations and X-ray crystallographic data [3,9], in the unit cell of (S)-IBP (or (R)-IBP) the molecules in the dimer are in different conformational state, though both in the (S)- (or (R)-) configuration. In contrast, the racemate IBP dimer is formed by hydrogen bonds across a centre of inversion, with one molecule in the (R)- configuration, and the other in the (S)-configuration (figure 3). As a consequence, the surrounding environment "seen" by the carbonyl groups, to which the C=O stretching mode is strongly sensitive, is similar for the two enantiomers but different with respect to the racemate.

[Insert figure 3 about here]

In figure 4 we report the FTIR-ATR spectra of the inclusion complexes formed by Me-β-CD with (R, S)-, (R)- and (S)-IBP. As can be seen, the three complexes exhibit a markedly different vibrational behaviour.

[Insert figure 4 about here]

In particular, we observe, in the case of (S)-IBP/Me-β-CD, an enhanced intensity of the δ-HOH bending mode of water molecules attached to the Me-β-CD, revealed at ~ 1640 cm^{-1}. As reported in literature [23], the intensity of band related to intramolecular HOH bending mode of bulk liquid water diminishes with decreasing temperature and tends to zero at the crystallization. So, bending band can be ascribed to the water molecules not involved in a symmetric tetrahedral network. This

occurrence, then, lets us hypothesize, for the (S)-IBP/Me-β-CD case, the presence of a major number of crystallization water molecules, in molecular form, still present inside the cavity even after complexation.

For a quantitative analysis of the vibrational contributions in this spectral region, curve-fitting techniques has been used, with the wavenumber of the maxima of the band components evalutated from second derivative computations. The fit turned out to be as realistic as possible by using three components, at ~ 1640 cm^{-1} (δ-HOH bending of water molecules attached to β-CDs), at ~ 1710 cm^{-1} (C=O stretching of uncomplexed dimeric IBP) and at ~ 1730 cm^{-1} (C=O stretching of complexed monomeric IBP), as minimum number of bands corresponding to the number of distinct features observed in the experimental spectra. The partial overlapping of the δ-HOH bending and C=O stretching vibrations has been solved by simultaneously fitting, in a first step, the whole spectrum, and, then, by subtracting the contribution at ~ 1640 cm^{-1} and performing a more detailed fit for the C=O stretching mode. In this last case, two components have been necessary for a realistic reproduction of the experimental spectra, ω_1 at ~ 1710 cm^{-1} and ω_2 at ~ 1730 cm^{-1}, ascribed, respectively, to the C=O stretching of uncomplexed and complexed IBP. The final deconvolutions of the C=O stretching band for (R)-IBP/Me-β-CD and (S)-IBP/Me-β-CD inclusion complexes are shown in figure 5(a-b), at T = 300 K as an example, and the main deconvolution data (wavenumbers and percentage areas) are given in table 1.

[Insert figure 5 about here]

[Insert table 1 about here]

We observe a tendency of the wavenumbers of each component to shift to higher values by increasing temperature, ascribed to a strengthening of the double bond in the corresponding carbonyl groups because of the establishment of weaker forces.

The temperature-dependence of percentage intensities of IR bands, which are representative, as well known, of the population of the corresponding oscillators, has been described according to a model already successfully applied in the case of (R, S)-IBP/β-CDs inclusion complexes.[18, 24] Once the thermal reversibility of the inclusion complex has been checked, an "affinity" constant $A(T)$ has been introduced, defined as:

$$A(T) = \frac{I_2(T)}{I_1(T)} = \frac{n_2(T)}{n_1(T)}, \qquad (1)$$

where $n_1(T)$ and $n_2(T)$ are, respectively, the number of uncomplexed and complexed IBP molecules at a given temperature T.

$A(T)$ was found to decrease with increasing temperature according to the equation:

$$\ln A = \left(\frac{-\Delta H}{RT} \right) + \frac{\Delta S}{R}, \qquad (2)$$

being ΔH and ΔS the enthalpy and entropy variations associated with the binding of IBP and Me-β-CD in solid phase, respectively, and R the gas constant.

From the slope of the linear plot of the logarithm of $A(T)$ as a function of inverse temperature, shown in figure 6(a-b), we estimated ΔH = -5797 ± 283 J·mol^{-1} for (R)-IBP/Me-β-CD and ΔH = -4272 ± 224 J·mol^{-1} for (S)-IBP/Me-β-CD inclusion complexes, respectively.

[Insert figure 6 about here]

The large and negative obtained ΔH values are comparable with those already obtained for (R, S)-IBP/Me-β-CD inclusion complex (ΔH = -3573 ± 317 J·mol^{-1}, as reported in ref. [18]). Then, a similar complexation mechanism for both racemic and enantiomeric IBP can be hypothesized, driven by the breaking down of intermolecular hydrogen bonding of dimeric IBP, the release of enthalpy-rich water molecules from the hydrophobic cavity of CD, their replacement with monomeric IBP molecules, and the rearrangement of crystallization H_2O in a new H-bond environment. Nevertheless, enantiomers are shown to form, in solid phase, more stable inclusion complex with respect to the racemate. This is in agreement with what revealed by Nerurkar et al. [16], in liquid phase, by solubility studies on (R, S)-IPB and (S)-IBP inclusion complexes with hydroxypropyl (HP) β-CDs, and can be justified thinking that the intermolecular dimeric H-bond between one (R)-IBP molecule-and one (S)-IBP molecule, taking place in the racemate, is favoured with respect to the H-bond developed between two IBP molecules in the (R)- or (S)- configuration. Hence, it is more difficult to be broken, and this occurrence makes the complexation process in the (R, S)-IBP/Me-β-CD system, in a way, hindered. This interpretation can be supported also by the value of the total energies computed at DFT level for (R, S)- and (R)-IBP dimers, where the energy for racemic IBP results lower of about 0.46 kcal/mol respect to (R)-IBP, in agreement with other molecular mechanics computations. [3]

4. Conclusions

A quantitative analysis about the influence of chirality on the spectroscopic modifications induced, in solid phase, on the C=O stretching vibration of inclusion complexes formed by enantiomers and racemate of IBP with Me-β-CD has been performed, by the combined use of FTIR-ATR spectroscopy and numerical simulation. By exploring a wide temperature range, from 250 K to 340 K, we have been able to furnish a description of the complexation mechanism, quantifying, as main

contribution, the enthalpy changes associated to the "host-guest" interaction. A higher stability has been revealed in the case of the complexes formed by the enantiomers with respect to racemate. It has been ascribed to the increased difficulty, in this last case, in breaking the intermolecular dimeric hydrogen bond between (R)- and (S)-IBP molecules, proved to constitute the first step for complexation.

References

[1] J. C. Leffingwell, Leffingwell Rep. **3** 1 (2003).

[2] S. S. Adams, P. Bresloff and C. Manson, J. Pharm. Pharmacol. **28** 256 (1976).

[3] S. Bogdanova, I. Pareva, P. Nikolova, I. Tskavoska and B. Muller, Pharm. Res. **22** 806 (2005).

[4] Z. Li, M. Zell, E. Munson and D. Grant, J. Pharm. Sci. **88** 337 (1999).

[5] G. Pelrovich, S. Kurkov, L. Hansen and A. Bauer-Brand, J. Pharm. Sci. **93** 654 (2004).

[6] N. Shankland, C. Wilson, A. Florence and P. Cox, Acta Crystallogr. **C53** 951 (1997).

[7] K. Shankland, W. David, T. Csoka and L. McBride, Int. J. Pharm. **165** 117 (1998).

[8] N. Shankland, A. Florence, P. Cox, C. Wilson and K. Shankland, Int. J. Pharm. **165** 107 (1998).

[9] A. Freer, J. Bunyan, N. Shankland and D. Sheen, Acta Crystallogr. **C49**, 1378 (1993).

[10] J. McConnell, Cryst. Struct. Comm. **3** 73 (1974).

[11] N. Okulik and A. Jubert, J. Mol. Struct. **769** 135 (2006).

[12] J. Reijenga, B. Inglese and F. Everaerts, J. Chromatogr. A **792** 371 (1997).

[13] S. La, J. Kim, J. Goto and K. Kim, Electrophor. **24**, 2642 (2003).

[14] K. Busch, I. Swamidoss, S. Fakayode and M. Busch, Anal. Chim. Acta **525** 53 (2004).

[15] M. Blanco, J. Coello, H. Iturriaga, S. Maspoch and C. Perez-Maseda, J. Chromatogr. A **793** 165 (1998).

[16] J. Nerurkar, J. Beach, M. Park and H. Jun, Pharm. Dev. Technol. **10**, 413 (2005).

[17] C. J. Nunez-Aguero, C. M.Escobar-Llanos, D. Diaz, C. Jaime and R. Garduno-Juarez, Tetrahedron 62, 4162 (2006)

[18] V. Crupi, G. Guella, D. Majolino, I. Mancini, B. Rossi, R. Stancanelli, V. Venuti, P. Verrocchio, G. Viliani, J. Phys. Chem. A (2010) (in press).

[19] B. Rossi, P. Verrocchio, G. Viliani, I. Mancini, G. Guella, E. Rigo, G. Scarduelli, G. Mariotto, J. Raman Spectrosc. **40,** 453 (2009).

[20] M. J. Frisch, G. W. Trucks, H. B. Schlegel, G. E. Scuseria, M. A. Robb, J. R. Cheeseman, J. A. Montgomery, T. Vreven Jr, K. N. Kudin, J. C. Burant, J. M. Millam, S. S. Iyengar, J. Tomasi, V. Barone, B. Mennucci, M. Cossi, G. Scalmani, N. Rega, G. A. Petersson, H. Nakatsuji, M. Hada, M. Ehara, K. Toyota, R. Fukuda, J. Hasegawa, M. Ishida, T. Nakajima, Y. Honda, O. Kitao, H. Nakai, M. Klene, X. Li, J. E. Knox, H. P. Hratchian, J. B. Cross, C. Adamo, J. Jaramillo, R. Gomperts, R. E. Stratmann, O. Yazyev, A. J. Austin, R. Cammi, C. Pomelli, J. W. Ochterski, P. Y. Ayala, K. Morokuma, G. A. Voth, P. Salvador, J. J. Dannenberg, V. G. Zakrzewski, S. Dapprich, A. D. Daniels, M. C. Strain, O. Farkas, D. K. Malick, A. D. Rabuck, K. Raghavachari, J. B. Foresman, J. V. Ortiz, Q. Cui, A. G. Baboul, S. Clifford, J. Cioslowski, B. B. Stefanov, G. Liu, A. Liashenko, P. Piskorz, I. Komaromi, R. L. Martin, D. J. Fox, T. Keith, M. A. Al-Laham, C. Y. Peng, A. Nanayakkara, M. Challacombe, P. M. W. Gill, B. Johnson, W. Chen, M. W. Wong, C. Gonzalez and J. A. Pople, Gaussian 03 (Revision A.10), Gaussian, Inc., Pittsburgh, PA (2003).

[21] C. Lee, W. Yang and R. G. Parr, Phys. Rev. B **37** 785 (1988).

[22] A. D. Becke, J. Chem. Phys. **98** 5648 (1993).

[23] J. B. Brubach, A. Mermet, A. Filabozzi, A. Gerschel and P. Roy, J. Chem. Phys. **122** 184509 (2005).

[24] V. Crupi, G. Guella, D. Majolino, I. Mancini, B. Rossi, R. Stancanelli, V. Venuti, P. Verrocchio and G. Viliani, J. Mol. Struct. **972** 75 (2010).

T (K)	ω_1 (cm^{-1})	I_1 (%)	ω_2 (cm^{-1})	I_2 (%)
(R)-IBP/Me-β-CD inclusion complex				
250	1701.5	48.9	1726.4	51.1
260	1704.1	53.1	1727.8	46.9
270	1705.9	54.8	1728.5	45.2
280	1707.2	55.4	1729.1	44.6
290	1707.7	58.0	1729.5	42.0
300	1709.7	61.4	1730.2	38.6
310	1710.2	63.6	1730.4	36.4
320	1710.0	64.4	1730.9	35.6
330	1711.9	65.9	1731.1	34.1
340	1712.2	66.4	1731.1	33.6
(S)-IBP/Me-β-CD inclusion complex				
250	1700.1	56.1	1725.2	43.9
260	1702.5	56.5	1727.3	43.4
270	1703.4	59.8	1727.6	40.2
280	1705.6	61.8	1728.6	38.2
290	1706.9	62.8	1728.6	37.2
300	1706.6	64.5	1729.2	35.5
310	1708.2	65.6	1730.1	34.4
320	1708.6	67.1	1730.8	32.8
330	1709.7	67.4	1730.4	32.6
340	1710.9	67.6	1731.2	32.3

Table 1 – Best-fit results for C=O stretching band for (R)-IBP/Me-β-CD and (S)-IBP/Me-β-CD inclusion complexes.

Figure captions

Figure 1 – Structure of the two enantiomers of IBP: (a) (R)-IBP, (b) (S)-IBP. Notation: full wedge: bond outgoing, empty wedge: bond ingoing.

Figure 2 – FTIR-ATR spectra, at T = 300 K, in the 600 ÷ 3800 cm^{-1} wavenumber range, of ((a), solid line) (R, S)-, ((b), closed squares) (R)-, and ((c), open circles) (S)-IBP. In the inset, the C=O stretching region (1500 ÷ 1800 cm^{-1}) for the same systems is reported.

Figure 3 – Minimized structure for dimers of (R,S)-IBP (at the top) and (R)-IBP (at the bottom). Atoms in red indicate the oxygens involved in the hydrogen bonding interaction.

Figure 4 – FTIR-ATR spectra, at T = 300 K, in the C=O stretching region (1500 ÷ 1800 cm^{-1}), of (R, S)-IBP/Me-β-CD (solid line), (R)-IBP/Me-β-CD (closed squares), (S)-IBP//Me-β-CD (open circles) inclusion complexes.

Figure 5 – The fit of the FTIR-ATR band in the 1650 ÷ 1760 cm^{-1} wavenumber range of (R)-IBP/Me-β-CD (a) and (S)-IBP/Me-β-CD (b) inclusion complex, at T = 300 K. Continuous line: best-fit, dashed lines: deconvolution components.

Figure 6 - Semi-log plot of A vs. 1/T for (a) (R)-IBP/Me-β-CD and (b) (S)-IBP/Me-β-CD inclusion complex, together with the best-fit performed according to equation (2). See text for details

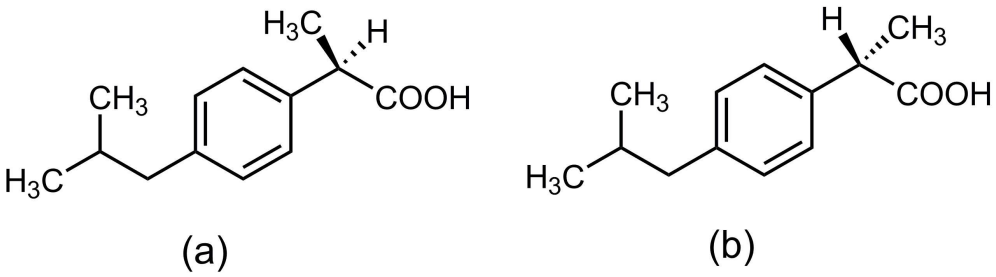

Figure 1
109x30mm (600 x 600 DPI)

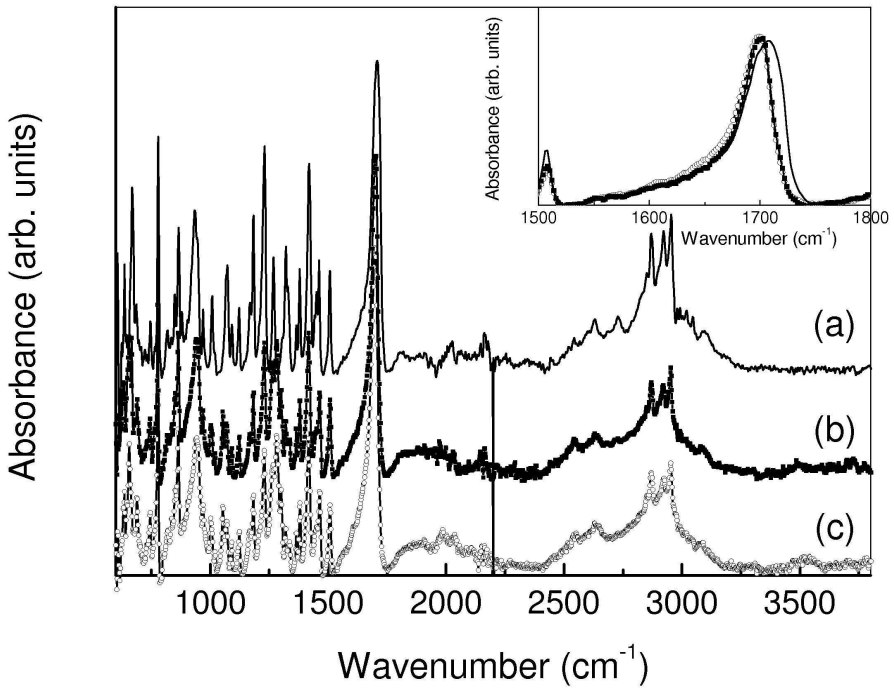

Figure 2
102x81mm (600 x 600 DPI)

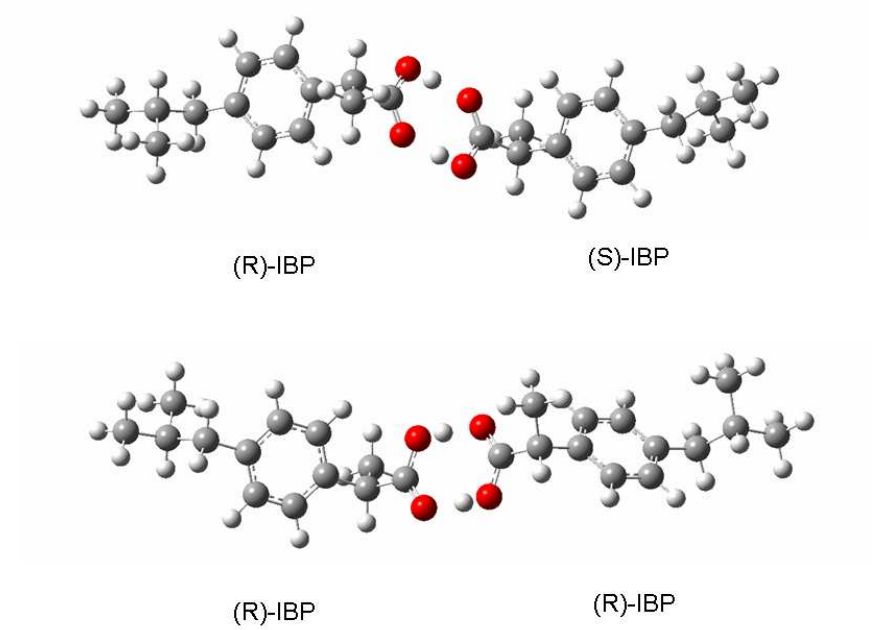

Figure 3
254x190mm (96 x 96 DPI)

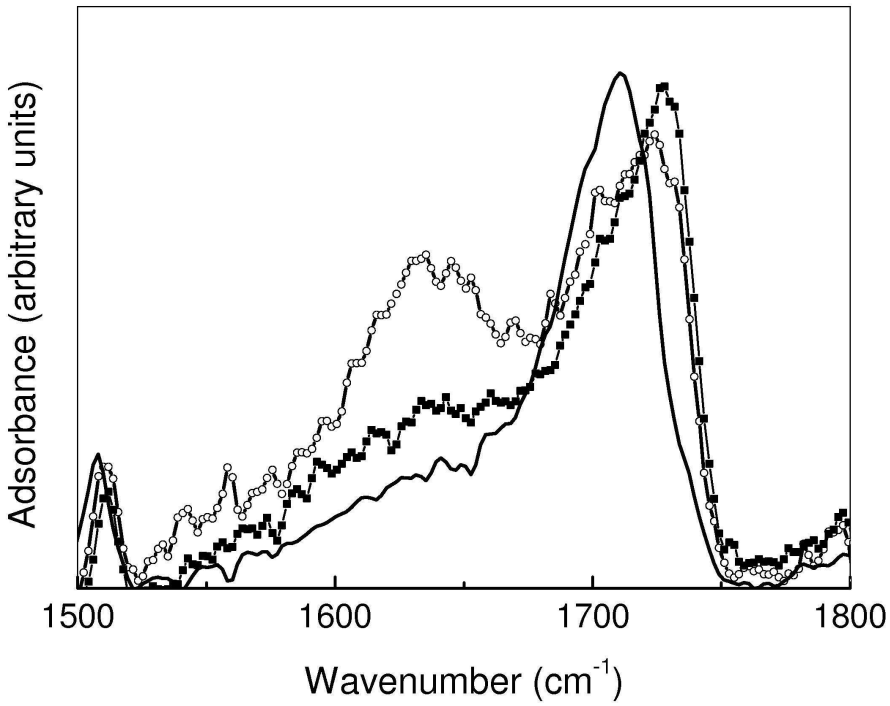

Figure 4
100x81mm (600 x 600 DPI)

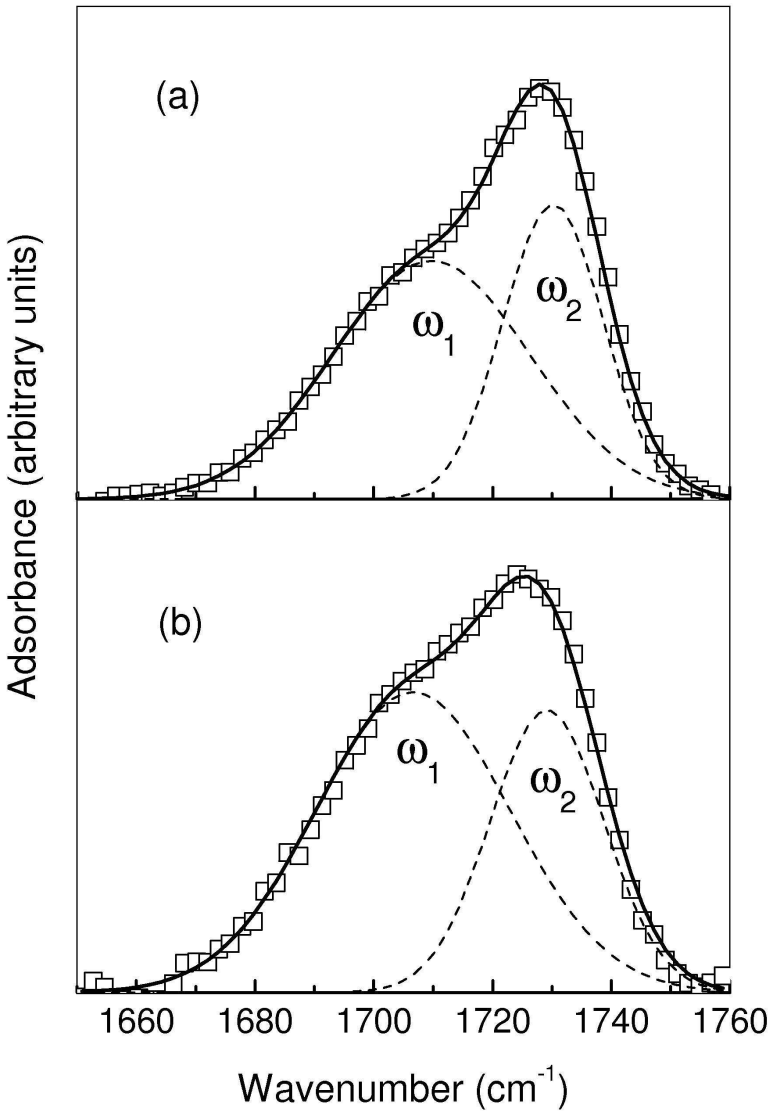

Figure 5
82x115mm (600 x 600 DPI)

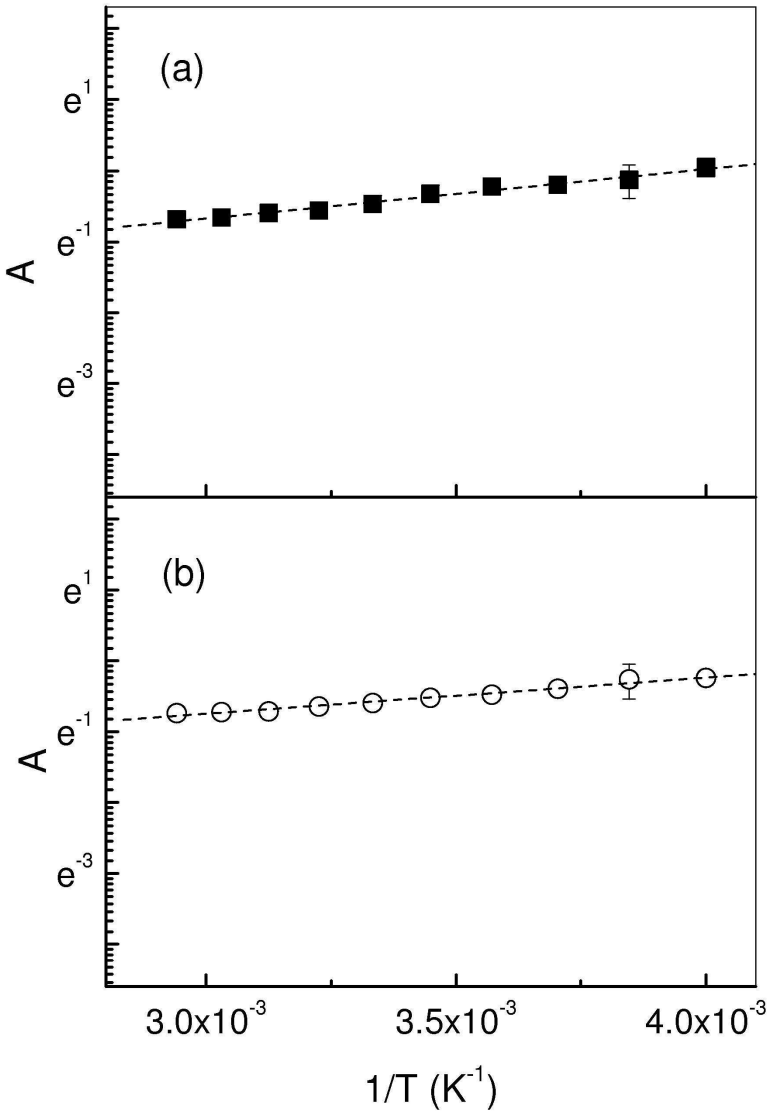

Figure 6
83x116mm (600 x 600 DPI)